Title

Housing environment bilaterally alters transcriptomic profile in the rat hippocampal CA1 region

Authors

Azusa Kubota[1], Kentaro Kojima[2], Shinnosuke Koketsu[3], Takayuki Kannon[2,4], Takehiro Sato[2,5], Kazuyoshi Hosomichi[2,6], Yoshiaki Shinohara[7,*], Atsushi Tajima[1,2,*]

[1]Department of Bioinformatics and Genomics, Graduate School of Advanced Preventive Medical Sciences, Kanazawa University, Kanazawa, Japan

[2]Department of Bioinformatics and Genomics, Graduate School of Medical Sciences, Kanazawa University, Kanazawa, Japan

[3]Department of Physical Therapy, Faculty of Medical Science, Nagoya Women's University, Nagoya, Japan

[4]Department of Biomedical Data Science, Fujita Health University, School of Medicine, Toyoake, Japan

[5]Department of Human Biology and Anatomy, Graduate School of Medicine, University of the Ryukyu, Nishihara, Japan

[6]Laboratory of Computational Genomics, School of Life Science, Tokyo University of Pharmacy and Life Sciences, Tokyo, Japan

[7]Department of Anatomy and Systems Biology, Faculty of Medicine, University of Yamanashi, Yamanashi, Japan

*Co-corresponding authors:

Atsushi Tajima, Ph.D.

Department of Bioinformatics and Genomics, Graduate School of Medical Sciences, Kanazawa University, 13-1 Takara-machi, Kanazawa 920-8640, Japan

Fax: +81-76-234-4249; Phone: +81-76-265-2715

E-mail: atajima@med.kanazawa-u.ac.jp

Yoshiaki Shinohara, M.D., Ph.D.

Department of Anatomy and Systems Biology, Faculty of Medicine, University of Yamanashi, 1110 Shimokato, Chuo, Yamanashi 409-3898, Japan

Fax: +81-55-273-9473; Phone: +81-55-273-9471

E-mail: yoshinohara@yamanashi.ac.jp

Abstract

Brain asymmetry is widely observed in different species. Studies on rodent hippocampi have provided morphological and physiological explanations for left-right asymmetry and have

shown that the environment influences hippocampal lateralization in the CA1 region. However, how the left-right asymmetry arises, and its significance are not fully understood. In this study, we aimed to elucidate the transcriptome profiles of the rat hippocampus associated with lateralization and to assess the sensitivity of the bilateral CA1 region to an enriched environment. Transcriptomic analysis using RNA-seq was performed on the left and right CA1 regions of male rats reared in isolated or enriched environments. Although differentially expressed genes (DEGs) were not found between left and right CA1 under either environmental condition, environment-induced DEGs were significantly detected in both left and right CA1. DEGs common to both hemispheres were also found in the environmental comparison, and immediate early genes were suggested as relevant together with gene co-expression network analysis. Gene set enrichment analysis revealed that the profiles of gene expression change due to the enriched environment in the bilateral CA1 were significantly enriched in the suppressed direction in several gene sets, including those related to synaptic signaling and organization, and neuronal connection.

Introduction

Numerous animals, including humans, have left-right asymmetric brains and in humans and primates, the acquisition of higher brain functions is closely related to brain asymmetry [1,2]. Electroencephalogram (EEG) and functional magnetic resonance imaging (fMRI) characterize

the time- and space-dependent functional differences between the left and right cerebrum of the human brain [3]. Those functional differences are thought of as various responses to environmental stimuli such as task performance and stress exposure. Although the lateral specialization of the brain has been extensively studied, the molecular factors and intricate mechanisms remain largely unknown.

Studies of hippocampal asymmetry suggest that the genetic mechanisms of visceral and brain lateralization are different. Chiral movement of the cilia induces leftward nodal flow during embryonic development and consistently produces a predictable asymmetry in the arrangement of thoracic and abdominal organs in adulthood [4]. Normal ciliary function in wild-type mice is associated with an uneven hippocampus, and the disruption of ciliary motility leads to the randomization of organ laterality. In mice with arbitrarily inhibited ciliary movements, bilateral right isomerism occurs in the hippocampal circuitry regardless of the original direction of organ laterality [5]. Interestingly, molecular variations in the brain are sometimes driven by specific gene expression patterns in the body. For example, the *iv* mouse, which has a mutation in the *Lrd* (left-right dynein) gene, disrupt organ lateralization and abolish hippocampal lateralization, ultimately resulting in spatial reference and working memory deficits [6].

In rodents, synaptic sizes differ between CA1 pyramidal cell synapses when receiving input from the left and right CA3 pyramidal cells, and the expression pattern of the glutamate

receptor subunit is associated with synapse size [7,8]. Additionally, individual environmental experiences can induce hippocampal asymmetry in the CA1 region. Rats reared in an enriched environment with running wheels, tunnels, and toys, exhibit increased synaptic density in the right CA1, and increased interhemispheric gamma coherence [9]. The results suggest that an enriched environment shapes the functional asymmetry of hippocampal circuitry through synaptic reorganization. Lateralization induced by environmental factors has been studied in several animal models and at different levels, including zebrafish, avians, and humans [10,11]. For a comprehensive understanding of neural asymmetry and its formation, it is also worth highlighting the relationship between environmental factors and changes in gene expression in the rodent hippocampus.

Differential mRNA profiles between the whole left and right rat hippocampi have been observed using microarrays [12], and interhemispheric differences in microRNA profiles have been found using rat hippocampal CA3 region [13]. However, the genes responsible for neurological laterality in the rodent hippocampus and the influence of the environment remain unknown. Therefore, in this study, we aimed to elucidate the transcriptomic profile of the left and right CA1 regions and assess their respective sensitivity to an enriched environment using RNA-seq.

Materials and Methods

Animals and microdissection

Male Long-Evans rats were reared under isolated (ISO) or enriched (ENR) conditions. The ISO group was caged individually after weaning at 21 days of age and raised in standard cages (length, 32 cm; width, 22 cm; height, 13.5 cm). In the ENR group, five to six male littermates were housed together in a larger cage (length 44 cm, width 27 cm, height 18.7 cm) with a ladder, running wheels, tunnels, and toys, the location of which was changed every 3–4 days. Hippocampal slices were prepared 4 weeks after rearing in the two environmental conditions as previously described [7,8,13]. Briefly, the rats were euthanized and their brains were immediately washed with ice-cold ACSF. After cooling in ACSF for 15 min, the hippocampal slices were cut into 400-µm-thick sections using a Mcllwain tissue chopper. The bilateral rat CA1 regions were manually dissected under a stereoscopic microscope (Olympus, Japan) using a handmade microblade. Three biological replicates were prepared for sequencing from both the left and right CA1. The study design was approved by the Animal Experimental Committee of Nagoya City University (Approval number: H29M-44). The protocol of the current animal study was in accordance with the ARRIVE guidelines 2.0 (https://arriveguidelines.org).

Library preparation and RNA-seq

Total RNA was extracted from rat CA1 region tissues using the RNeasy® Mini Kit (Qiagen, Germany), according to the manufacturer's protocol. All RNA samples exhibited an

appropriate range of RNA integrity number (RIN) values, which were measured using a Bioanalyzer (Agilent, USA). The cDNA libraries for RNA-seq were prepared from 500 ng of extracted RNA using the TruSeq® Stranded mRNA Sample Preparation Kit (Illumina, USA), according to the manufacturer's instructions. The libraries were sequenced on an Illumina HiSeq2000 to obtain 101-bp paired-end reads for each sample.

Computational quantification of gene expression

Sequenced reads were processed using fastp [14] (version 0.22.0) to eliminate low-quality reads and trim the adapter sequences. Transcript quantification was performed using Salmon [15] (version 0.8.1) with Ensembl mRatBN7.2 cDNA assembly. Salmon output files were converted into read-count data and summarized from transcript-level to gene-level quantification by using tximport [16] (version 1.28.0). The converted raw gene count data were normalized using tximport with the TPM (transcripts per million) method for clustering analysis. Hierarchical clustering was performed to summarize the similarity of the samples focusing on Pearson's correlation.

Differentially expressed genes analysis

Statistical calculations of differentially expressed genes (DEGs) were performed with edgeR [17-19] (version 4.4.0). After filtering the very low expressed genes with the filterByexpr()

function, two-dimensional scatter plots were drawn with the plotMDS() function. Quasi-likelihood F-test (QLF) was used to evaluate the significance of gene expression level. An appropriate design matrix was formulated for the left-right sample-paired QLF. Nominal *p*-values were adjusted using false discovery rate (FDR) correction. In this step, the left group was treated as the control in the left-right comparison, and the ISO group was treated as the control in the ISO-ENR comparison. DEGs were detected using arbitrary thresholds of FDR = 0.05 and $\log_2$(fold-change) = $\pm\log_2 1.5$ (= ±0.58). A correlation plot was created for the environmental comparisons of left and right CA1 using the $\log_2$(fold-change) ($\log_2$FC) values of the 10,684 common genes after filtering.

RT-qPCR

Reverse transcription reaction was performed by using ReverTra Ace® qPCR RT Master Mix (TOYOBO, Japan). The PCR mixture was prepared with 10.0 µL of THUNDERBIRD® Next SYBR qPCR Mix (TOYOBO, Japan), 0.3 µM of forward and reverse primer, 1.0 µL of cDNA, and 7.8 µL of sterilized water. QuantStudio 6 Pro (Applied Biosystems, USA) was used for qPCR analysis. A relative quantification method [20] was used to measure the amount of each gene using *Gapdh* as a normalizer. Details of the primer sequences used are in Table 1. Welch's t-test was performed between ISO and ENR using the ΔCt values.

Gene co-expression network analysis

Cytoscape [21] (version 3.10.2) and geneMANIA [22] (version 3.5.3) were used to analyze the gene co-expression network in the overlapping DEGs between the environmental comparison of the left and right hemispheres. In addition to the input genes, the top 15 highly correlated genes were extracted and visualized together in the network using query gene-based weighting.

Gene set enrichment analysis

Gene set enrichment analysis (GSEA) [23] was performed in the environmental comparison data using clusterProfiler [24-26] (version 4.14.4) and fgsea [27] (version 1.32.0) with org.Rn.eg.db (version 3.20.0) as the genomic annotation. Gene Ontology (GO) was used to characterize the biological features of the gene sets. The $\log_2$FC values calculated by edgeR were used with the input information. Note that the parameters were optimized to describe the biological characterization of each condition. Benjamini-Hochberg correction was used to adjust the *p*-values to control the false-discovery rate. The parameters involved in the filtering used are as follows: Conditions of the left ISO-ENR comparison: ont = "ALL", minGSSize = 10, maxGSSize = 520, pvalueCutoff = 0.05; Conditions of right ISO-ENR comparision: ont = "ALL", minGSSize = 10, maxGSSize = 615, pvalueCutoff = 0.1.

Data processing, statistics, and drawing

R (version 4.4.2) was used for data handling, statistical computing, and data visualization.

Results

Comparison of transcriptomic similarity

Hierarchical clustering method was used to characterize the similarity between samples based on TPM-normalized data in a dendrogram (Fig 1). The dendrogram was largely divided into ENR and ISO, and the left and right CA1 data from the same individual showed paired structures. The TPM-normalized gene count data are in S1 Data.

Differentially expressed genes analysis and RT-qPCR

The multidimensional scaling (MDS) plots showing the relationships between samples generated after data preprocessing with edgeR are shown in S1 Fig. DEG analysis showed no significant genes that met the criteria in the left-right comparison of both ISO and ENR conditions (S2 Fig). On the other hand, the ISO-ENR comparison revealed significant differences in the gene expression profile in both left and right CA1. 105 genes were detected as DEGs in the left CA1 group; 9 genes were highly expressed in ENR and 96 genes were highly expressed in ISO (Fig 2A). 13 genes were detected as DEGs in the right CA1 group; only 1 gene was highly expressed in ENR and 12 genes were highly expressed in ISO (Fig

2B). The data of the DEG lists are in S2 Data. The correlation plot of $\log_2$FC values for the environmental comparisons of left and right CA1 yielded a Pearson's correlation coefficient of 0.626 (S3 Fig). The number of overlapping ISO-ENR DEGs between left and right CA1 was visualized in Fig 2C. 7 DEGs were shared and all of them were highly expressed in ISO (Table 2). To validate the DEG analysis results, *Cdkl5* and *Fos* were selected from Table 2 to perform RT-qPCR. These target genes were selected according to the following criteria: $\log_{10}$CPM > 2.5 and $\log_2$FC < 1.5. *Cdkl5* and *Fos* showed significantly lower relative expression in ENR compared to ISO in both left and right CA1 groups (Fig 3).

Gene co-expression network of left-right overlap DEGs in environmental comparison

The 7 overlapping DEGs were further used to characterize the environmentally induced gene expression profile in bilateral CA1. The result of gene co-expression network analysis was visualized in Fig 4. Based on the geneMANIA algorithm, the co-expression network was explained, and 15 genes were additionally expected to be as co-expressed genes. Among the 15 genes, only *Egr1* was included in the ISO-ENR DEG list of the left CA1; the other genes were not found in the lists of any ISO-ENR DEG analysis results. The details of this result are in S3 Data.

Gene ontology gene set enrichment analysis in environmental comparison

For biological interpretation of the environmental effect, the gene lists ranked by their corresponding $\log_2$FC values were further analyzed. The dot plots in Fig 5 show the results of GSEA focusing on the environmental condition in the left and right CA1 groups. Note that each direction of GO enrichment was evaluated using $\log_2$FC values as input information. In total, 43 gene sets were enriched in the left ISO-ENR, and 16 gene sets were enriched in the right ISO-ENR. In the left ISO-ENR, all the significant gene sets were evaluated as suppressed, except for the respiratory chain complex gene set. In the right ISO-ENR, all the significant gene sets were found to be suppressed. Finally, enrichment profiles were visualized to represent the enrichment pattern for particular gene sets using the Enrichment Score and the $\log_2$FC values (S4 Fig). All the results are in S4 Data.

Discussion

In this study, transcriptomic approaches revealed the extent of left-right differential gene expression and the influence of enriched environment in the bilateral CA1 region. DEG analysis revealed the environment-induced gene expression signatures in the left and right CA1 (Fig 2A and B). Focusing on the $\log_2$FC values and the number of ISO-ENR DEGs in each left and right CA1 region, it is suggested that the influence of the housing environment is

lateralized at the transcriptome level in the hippocampal CA1, while the direction of transcript regulation is significantly correlated overall (S3 Fig). Of particular interest, the number of genes whose expression was significantly increased in the isolated environment was notably higher in the left CA1 (Fig 2A). On the other hand, we did not detect any DEGs between the left and right CA1 in either environment. This is consistent with the hierarchical clustering (Fig 1) and the MDS plots (S1 Fig), indicating that the differences in gene expression between the left and right CA1 regions are relatively smaller than those between the rearing environments. Future large-scale studies are needed to understand the details of the hippocampal left-right asymmetry at the gene expression level.

The bilaterally overlapping DEGs in the environmental comparison (Table 2) were highlighted by the Venn diagram (Fig 2C) and characterized by the co-expression network (Fig 4). Focusing on the network and DEG lists, only one expected co-expression gene, *Egr1*, was included in the ISO-ENR DEGs in the left CA1 group. *Egr1* is an immediately early gene (IEG) that acts as an initial response factor to external stimuli without protein synthesis and plays an important role in synaptic formation [28]. The same is true for *Fos*, which is an overlapping DEG. *Arc*, *Atf3*, *Fosb*, and *Nr4a1* are also the members of IEG, which were extracted as the candidates for co-expression genes in the network. The four genes were not statistically significant in our DEG analysis, but they may contribute to the transcriptomic signature we observed. On the other hand, an overlapping DEG, *Grin2b*, encodes one of the

NMDA receptor subunits of the glutamate receptor, also known specifically as the NR2B subunit. NMDA receptors play an important role in excitatory signaling in the central nervous system. Not only is it involved in synaptic plasticity and memory consolidation, but NR2B is also a key player in hippocampal asymmetry [7,8,13]. In addition, *Cdkl5*, which is another overlapping gene validated by RT-qPCR (Fig 3), is important for maintaining proper postsynaptic localization and function of NR2B-containing NMDA receptors in the hippocampus [29,30]. Note that in this study, it remains unclear why the overlapping genes mentioned here were highly expressed in the isolated environment. Further studies are required to understand this phenomenon.

GSEA in environmental comparison characterized the biological features in the left and right CA1 with the significant gene sets. Except for the respiratory chain complex gene set in the left ISO-ENR, all of the significant gene sets were scored as suppressed (Fig 5). This trend is thought to be related to the results of the DEG analysis and volcano plots (Fig 2A and B), where most of the DEGs were significantly expressed at lower levels in the enriched environment. Notably, the gene sets related to synaptic signaling (left: modulation of chemical synaptic transmission and regulation of trans-synaptic signaling, right: transmembrane receptor protein kinase activity and enzyme-linked receptor protein signaling pathway) and neuronal connection and synaptic organization (left: gene sets of neuron and synapse, right: gene sets of cell junction and adhesion) are both downregulated. This suggests

that although the total number of DEGs is quite different, the environment-induced transcriptomic profile and its direction are partially similar in the bilateral CA1. It would be interesting to hypothesize that stress or lack of experience in the isolated environment could activate the expression of some genes in the CA1 region.

Future studies, including integrated epigenomic-transcriptomic and other multi-omics analyses, will provide a better understanding of hippocampal left-right asymmetry and its environment-induced lateralization. On the other hand, it should be noted that this study has the following limitations. Careful consideration of sex differences in lateralization is needed in the future studies. We used male rats to exclude the possibility of female sex hormone influence on the laterality [9]. However, hippocampal asymmetry also occurs in female rats [31,32], and female-specific hippocampal asymmetry has been reported in the mouse model of temporal lobe epilepsy [33]. Although the present study used four weeks after weaning as the period of environmental exposure, this period should be carefully considered. Postnatal development of the brain, including the hippocampus, has a critical period associated with learning and experience [34,35]. Previous studies in mice have also examined the relationship between duration of environmental enrichment and subsequent structural and functional changes with hippocampal gene expression [36]. Cross-sectional studies over multiple time periods, including old age, are also important.

Acknowledgments

The authors thank Drs. Takatoshi Ueki and Hajime Hirase for their kind advice. The authors thank Ms. Yoko Iwauchi for her technical assistance.

Author contribution

YS and AT: conceptualization. AK, KK, SK, and KH: Investigation. KK and YS curated the data. AK and TS: Formal analysis. YS and AT: Funding Acquisition. YS and AT: resources. AK and AT: writing the original draft. AK, KK, SK, TK, TS, KH, YS, and AT: writing, reviewing, and editing.

Data availability

The RNA-seq dataset has been deposited in the Gene Expression Omnibus (GEO) of the National Center for Biotechnology Information under the accession number GSE270831. The other datasets are available from Supporting information of this article.

Funding information

This work was partially supported by JSPS KAKEN Grant Numbers JP17H02221 and JP20H03295 (to YS), and JP23K18386 and JP23H03145 (to AT). This work was also supported by JST SPRING, Grant Number JPMJSP2135 (to AK). This work included results

obtained using shared equipment under the MEXT Project for promoting public utilization of advanced research infrastructure (Program for supporting construction of core facilities) Grant Number JPMXS0440300024.

Additional information

The authors declare no competing interests.

Supporting information

S1 Fig. MDS plots after filtering the very low expression genes. (S1_Fig.pdf)

S2 Fig. Volcano plot visualizations of left-right comparison. (S2_Fig.pdf)

S3 Fig. Correlation plot of the $\log_2$FC values for the environmental comparisons in the left and right CA1. (S3_Fig.pdf)

S4 Fig. Enrichment profile visualization. (S4_Fig.pdf)

S1 Data. TPM-normalized gene count data. (S1_Data.xlsx)

S2 Data. DEG lists in ISO-ENR comparison. (S2_Data.xlsx)

S3 Data. Gene co-expression network analysis result. (S3_Data.xlsx)

S4 Data. Gene set enrichment analysis results in ISO-ENR comparison. (S4_Data.xlsx)

References

[1] Corballis MC. The evolution and genetics of cerebral asymmetry. Philos Trans R Soc Lond B Biol Sci. 2009;364(1519):867-79. doi: 10.1098/rstb.2008.0232. PubMed PMID: 19064358; PubMed Central PMCID: PMCPMC2666079.

[2] Corballis MC. Left brain, right brain: facts and fantasies. PLoS Biol. 2014;12(1):e1001767. Epub 20140121. doi: 10.1371/journal.pbio.1001767. PubMed PMID: 24465175; PubMed Central PMCID: PMCPMC3897366.

[3] Morillon B, Lehongre K, Frackowiak RS, Ducorps A, Kleinschmidt A, Poeppel D, et al. Neurophysiological origin of human brain asymmetry for speech and language. Proc Natl Acad Sci U S A. 2010;107(43):18688-93. Epub 20101018. doi: 10.1073/pnas.1007189107. PubMed PMID: 20956297; PubMed Central PMCID: PMCPMC2972980.

[4] Nonaka S, Shiratori H, Saijoh Y, Hamada H. Determination of left-right patterning of the mouse embryo by artificial nodal flow. Nature. 2002;418(6893):96-9. doi: 10.1038/nature00849. PubMed PMID: 12097914.

[5] Kawakami R, Dobi A, Shigemoto R, Ito I. Right isomerism of the brain in inversus viscerum mutant mice. PLoS One. 2008;3(4):e1945. Epub 20080416. doi: 10.1371/journal.pone.0001945. PubMed PMID: 18414654; PubMed Central PMCID: PMCPMC2291575.

[6] Goto K, Kurashima R, Gokan H, Inoue N, Ito I, Watanabe S. Left-right asymmetry defect in the hippocampal circuitry impairs spatial learning and working memory in iv mice. PLoS One. 2010;5(11):e15468. Epub 20101117. doi: 10.1371/journal.pone.0015468. PubMed PMID: 21103351; PubMed Central PMCID: PMCPMC2984506.

[7] Kawakami R, Shinohara Y, Kato Y, Sugiyama H, Shigemoto R, Ito I. Asymmetrical allocation of NMDA receptor epsilon2 subunits in hippocampal circuitry. Science. 2003;300(5621):990-4. doi: 10.1126/science.1082609. PubMed PMID: 12738868.

[8] Shinohara Y, Hirase H, Watanabe M, Itakura M, Takahashi M, Shigemoto R. Left-right asymmetry of the hippocampal synapses with differential subunit allocation of glutamate receptors. Proc Natl Acad Sci U S A. 2008;105(49):19498-503. Epub 20081203. doi: 10.1073/pnas.0807461105. PubMed PMID: 19052236; PubMed Central PMCID: PMCPMC2593619.

[9] Shinohara Y, Hosoya A, Hirase H. Experience enhances gamma oscillations and interhemispheric asymmetry in the hippocampus. Nat Commun. 2013;4:1652. doi: 10.1038/ncomms2658. PubMed PMID: 23552067; PubMed Central PMCID: PMCPMC3644069.

[10] Gunturkun O, Ocklenburg S. Ontogenesis of Lateralization. Neuron. 2017;94(2):249-63. doi: 10.1016/j.neuron.2017.02.045. PubMed PMID: 28426959.

[11] Gunturkun O, Strockens F, Ocklenburg S. Brain Lateralization: A Comparative Perspective. Physiol Rev. 2020;100(3):1019-63. doi: 10.1152/physrev.00006.2019. PubMed PMID: 32233912.

[12] Moskal JR, Kroes RA, Otto NJ, Rahimi O, Claiborne BJ. Distinct patterns of gene expression in the left and right hippocampal formation of developing rats. Hippocampus. 2006;16(8):629-34. doi: 10.1002/hipo.20198. PubMed PMID: 16847945.

[13] Shinohara Y, Yahagi K, Kawano M, Nishiyori H, Kawazu C, Suzuki N, et al. miRNA profiling of bilateral rat hippocampal CA3 by deep sequencing. Biochem Biophys Res Commun. 2011;409(2):293-8. Epub 20110514. doi: 10.1016/j.bbrc.2011.05.004. PubMed PMID: 21575607.

[14] Chen S, Zhou Y, Chen Y, Gu J. fastp: an ultra-fast all-in-one FASTQ preprocessor. Bioinformatics. 2018;34(17):i884-i90. doi: 10.1093/bioinformatics/bty560. PubMed PMID: 30423086; PubMed Central PMCID: PMCPMC6129281.

[15] Patro R, Duggal G, Love MI, Irizarry RA, Kingsford C. Salmon provides fast and bias-aware quantification of transcript expression. Nat Methods. 2017;14(4):417-9. Epub 20170306. doi: 10.1038/nmeth.4197. PubMed PMID: 28263959; PubMed Central PMCID: PMCPMC5600148.

[16] Soneson C, Love MI, Robinson MD. Differential analyses for RNA-seq: transcript-level estimates improve gene-level inferences. F1000Res. 2015;4:1521. Epub 20151230. doi:

10.12688/f1000research.7563.2. PubMed PMID: 26925227; PubMed Central PMCID: PMCPMC4712774.

[17] Robinson MD, McCarthy DJ, Smyth GK. edgeR: a Bioconductor package for differential expression analysis of digital gene expression data. Bioinformatics. 2010;26(1):139-40. Epub 20091111. doi: 10.1093/bioinformatics/btp616. PubMed PMID: 19910308; PubMed Central PMCID: PMCPMC2796818.

[18] Chen Y, Lun AT, Smyth GK. From reads to genes to pathways: differential expression analysis of RNA-Seq experiments using Rsubread and the edgeR quasi-likelihood pipeline. F1000Res. 2016;5:1438. Epub 20160620. doi: 10.12688/f1000research.8987.2. PubMed PMID: 27508061; PubMed Central PMCID: PMCPMC4934518.

[19] Chen Y, Chen L, Lun ATL, Baldoni PL, Smyth GK. edgeR v4: powerful differential analysis of sequencing data with expanded functionality and improved support for small counts and larger datasets. Nucleic Acids Res. 2025;53(2). doi: 10.1093/nar/gkaf018. PubMed PMID: 39844453; PubMed Central PMCID: PMCPMC11754124.

[20] Livak KJ, Schmittgen TD. Analysis of relative gene expression data using real-time quantitative PCR and the 2(-Delta Delta C(T)) Method. Methods. 2001;25(4):402-8. doi: 10.1006/meth.2001.1262. PubMed PMID: 11846609.

[21] Shannon P, Markiel A, Ozier O, Baliga NS, Wang JT, Ramage D, et al. Cytoscape: a software environment for integrated models of biomolecular interaction networks.

Genome Res. 2003;13(11):2498-504. doi: 10.1101/gr.1239303. PubMed PMID: 14597658; PubMed Central PMCID: PMCPMC403769.

[22] Warde-Farley D, Donaldson SL, Comes O, Zuberi K, Badrawi R, Chao P, et al. The GeneMANIA prediction server: biological network integration for gene prioritization and predicting gene function. Nucleic Acids Res. 2010;38(Web Server issue):W214-20. doi: 10.1093/nar/gkq537. PubMed PMID: 20576703; PubMed Central PMCID: PMCPMC2896186.

[23] Subramanian A, Tamayo P, Mootha VK, Mukherjee S, Ebert BL, Gillette MA, et al. Gene set enrichment analysis: a knowledge-based approach for interpreting genome-wide expression profiles. Proc Natl Acad Sci U S A. 2005;102(43):15545-50. Epub 20050930. doi: 10.1073/pnas.0506580102. PubMed PMID: 16199517; PubMed Central PMCID: PMCPMC1239896.

[24] Yu G, Wang LG, Han Y, He QY. clusterProfiler: an R package for comparing biological themes among gene clusters. OMICS. 2012;16(5):284-7. Epub 20120328. doi: 10.1089/omi.2011.0118. PubMed PMID: 22455463; PubMed Central PMCID: PMCPMC3339379.

[25] Wu T, Hu E, Xu S, Chen M, Guo P, Dai Z, et al. clusterProfiler 4.0: A universal enrichment tool for interpreting omics data. Innovation (Camb). 2021;2(3):100141. Epub

20210701. doi: 10.1016/j.xinn.2021.100141. PubMed PMID: 34557778; PubMed Central PMCID: PMCPMC8454663.

[26] Xu S, Hu E, Cai Y, Xie Z, Luo X, Zhan L, et al. Using clusterProfiler to characterize multiomics data. Nat Protoc. 2024;19(11):3292-320. Epub 20240717. doi: 10.1038/s41596-024-01020-z. PubMed PMID: 39019974.

[27] Korotkevich G, Sukhov V, Budin N, Shpak B, Artyomov MN, Sergushichev A. Fast gene set enrichment analysis. bioRxiv. 2021:060012. doi: 10.1101/060012.

[28] Kim S, Kim H, Um JW. Synapse development organized by neuronal activity-regulated immediate-early genes. Exp Mol Med. 2018;50(4):1-7. Epub 20180409. doi: 10.1038/s12276-018-0025-1. PubMed PMID: 29628504; PubMed Central PMCID: PMCPMC5938016.

[29] Okuda K, Kobayashi S, Fukaya M, Watanabe A, Murakami T, Hagiwara M, et al. CDKL5 controls postsynaptic localization of GluN2B-containing NMDA receptors in the hippocampus and regulates seizure susceptibility. Neurobiol Dis. 2017;106:158-70. Epub 20170706. doi: 10.1016/j.nbd.2017.07.002. PubMed PMID: 28688852.

[30] Okuda K, Takao K, Watanabe A, Miyakawa T, Mizuguchi M, Tanaka T. Comprehensive behavioral analysis of the Cdkl5 knockout mice revealed significant enhancement in anxiety- and fear-related behaviors and impairment in both acquisition and long-term retention of spatial reference memory. PLoS One. 2018;13(4):e0196587. Epub 20180427.

doi: 10.1371/journal.pone.0196587. PubMed PMID: 29702698; PubMed Central PMCID: PMCPMC5922552.

[31] Diamond MC, Murphy GM, Jr., Akiyama K, Johnson RE. Morphologic hippocampal asymmetry in male and female rats. Exp Neurol. 1982;76(3):553-65. doi: 10.1016/0014-4886(82)90124-8. PubMed PMID: 7084374.

[32] Wolff SC, Hruska Z, Nguyen L, Dohanich GP. Asymmetrical distributions of muscarinic receptor binding in the hippocampus of female rats. Eur J Pharmacol. 2008;588(2-3):248-50. Epub 20080409. doi: 10.1016/j.ejphar.2008.04.002. PubMed PMID: 18499095.

[33] Cutia CA, Leverton LK, Christian-Hinman CA. Sex and Estrous Cycle Stage Shape Left-Right Asymmetry in Chronic Hippocampal Seizures in Mice. eNeuro. 2023;10(6). Epub 20230605. doi: 10.1523/ENEURO.0041-23.2023. PubMed PMID: 37248046; PubMed Central PMCID: PMCPMC10249949.

[34] Sakai A, Sugiyama S. Experience-dependent transcriptional regulation in juvenile brain development. Dev Growth Differ. 2018;60(8):473-82. doi: 10.1111/dgd.12571. PubMed PMID: 30368782.

[35] Sakimoto Y, Shintani A, Yoshiura D, Goshima M, Kida H, Mitsushima D. A critical period for learning and plastic changes at hippocampal CA1 synapses. Sci Rep.

2022;12(1):7199. Epub 20220503. doi: 10.1038/s41598-022-10453-z. PubMed PMID: 35504922; PubMed Central PMCID: PMCPMC9065057.

[36] Singhal G, Morgan J, Jawahar MC, Corrigan F, Jaehne EJ, Toben C, et al. The effects of short-term and long-term environmental enrichment on locomotion, mood-like behavior, cognition and hippocampal gene expression. Behav Brain Res. 2019;368:111917. Epub 20190417. doi: 10.1016/j.bbr.2019.111917. PubMed PMID: 31004685.

Figure legends

Fig 1. Hierarchical clustering using the TPM-normalized gene count data.

The dendrogram shows the similarity of the samples using Pearson's correlation method among the normalized gene count data. ISO: isolated condition, ENR: enriched condition, L: left CA1, R: right CA1.

Fig 2. Differentially expressed genes of environmental comparison in left and right CA1.

A and **B** explain the distribution of statistically tested genes by volcano plot. FDR: false discovery rate, FC: fold-change. Thresholds for DEG analysis (FDR = 0.05 and $\log_2 FC = \pm \log_2 1.5$) are indicated by green dashed lines. **A.** ISO-ENR comparison in the left CA1. **B.** ISO-ENR comparison in the right CA1. **C.** The Venn diagram showing the relationship between each element of the left and right ISO-ENR DEG sets.

Fig 3. Gene expression of *Fos* and *Cdkl5* measured by RT-qPCR.

Gene expression of *Gapdh* was used for normalization. *$p < 0.05$, **$p < 0.01$, ***$p < 0.001$.

A. *Fos* gene expression. **B.** *Cdkl5* gene expression.

Fig 4. Gene co-expression network of bilaterally overlapping DEGs in the ISO-ENR condition and related genes.

The size of the node correlates with the score value, which reflects the degree of association with the network. The thickness of the edges reflects the association between nodes based on the weighting focused on the input genes. Note that some node positions have been manually moved to improve visibility. Red nodes: input genes. Blue nodes: related genes expected from the co-expression network. Red edges: connections among the input genes. Blue edges: the other connections.

Fig 5. Biological profile of environmental condition with gene set enrichment analysis.

In the ISO-ENR condition, Gene Ontology (GO) gene set enrichment analysis was performed using the genes subjected to edgeR analysis and their corresponding $\log_2$(fold-change) values. The top 10 significant gene sets were visualized, and each Gene Ratio value was described with

its associated GO terms. Adjusted *p*-values are shown below each dot. **A.** Dot plot in the left ISO-ENR. **B**. Dot plot in the right ISO-ENR.

Table 1. Primer information used in RT-qPCR.

Gene	Direction	Sequence
Gapdh	Forward	GGCACAGTCAAGGCTGAGAATG
	Reverse	ATGGTGGTGAAGACGCCAGTA
Fos	Forward	AGAAGGGGCAAAGTAGAGCAG
	Reverse	GCAGCCATCTTATTCCTTTCCC
Cdkl5	Forward	GTGGAAAGCAGCACACTGTC
	Reverse	CCTTGCTGTTGGATCTGTGATG

Table 2. Shared DEGs by comparing rearing environments in bilateral CA1.

Gene	Description	logCPM (L)	logFC (L)	FDR (L)	logCPM (R)	logFC (R)	FDR (R)
Cdkl5	cyclin-dependent kinase-like 5	2.75	-4.08	0.0207	2.91	-3.07	0.0102
Cds2	CDP-diacylglycerol synthase 2	6.20	-0.67	0.0261	6.14	-0.74	0.0264
Gabrb1	gamma-aminobutyric acid type A receptor subunit beta1	4.96	-0.84	0.0346	4.85	-0.82	0.0403
Grin2b	glutamate ionotropic receptor NMDA type subunit 2B	4.90	-1.41	0.00298	4.83	-1.13	0.0102
Gucy1a2	guanylate cyclase 1 soluble subunit alpha 2	3.54	-1.03	0.0181	3.55	-0.94	0.0442
Fos	Fos proto-oncogene, AP-1 transcription factor subunit	3.98	-1.79	0.00551	3.94	-1.87	0.0175
Kat6a	lysine acetyltransferase 6A	1.50	-9.53	0.0181	1.42	-9.41	0.0264

logCPM: $\log_{10}$CPM, logFC: $\log_2$(fold-change), FDR: false discovery rate.
L: left, R: right.

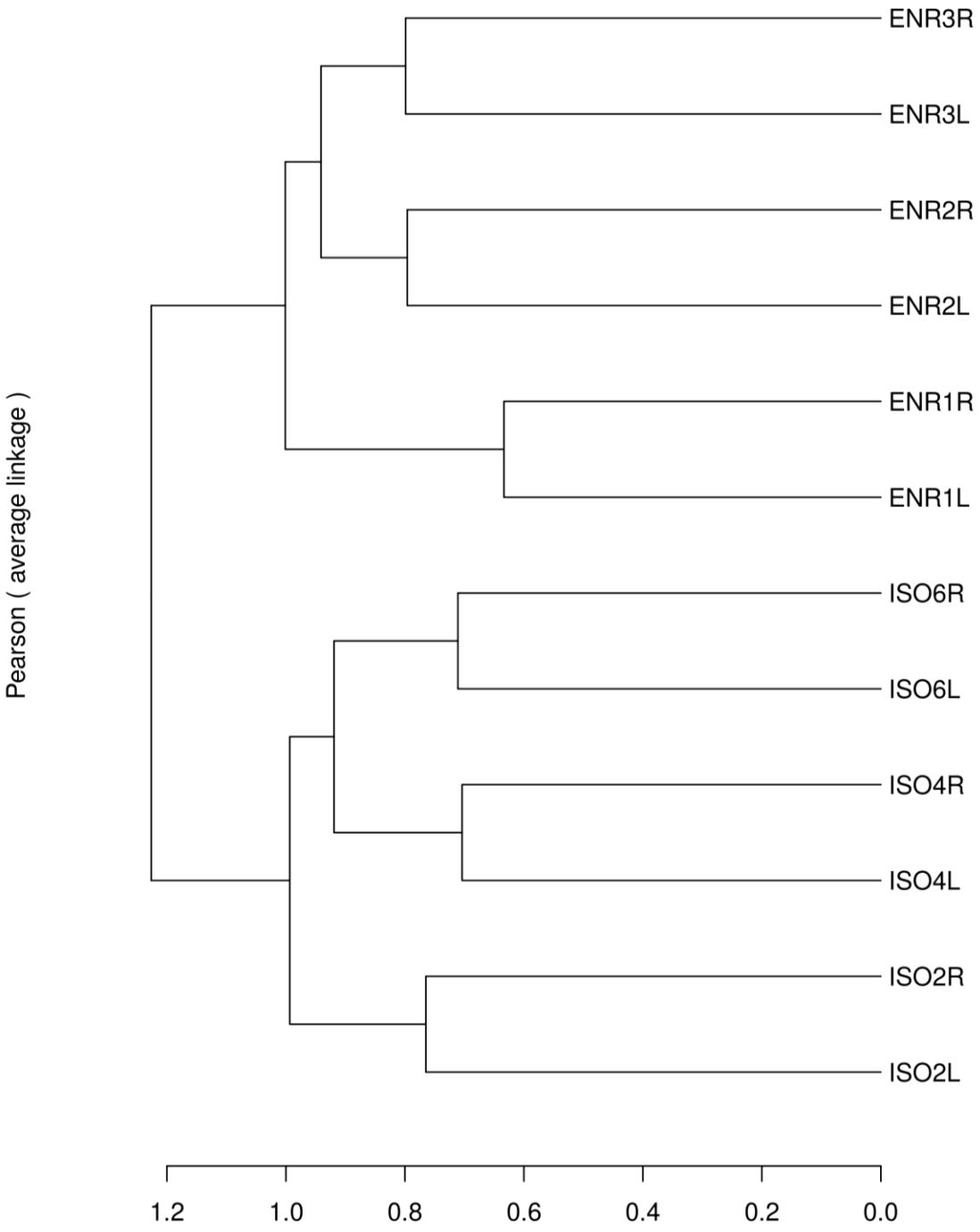
ENR3R
ENR3L
ENR2R
ENR2L
ENR1R
ENR1L
ISO6R
ISO6L
ISO4R
ISO4L
ISO2R
ISO2L
Pearson (average linkage)
1.2
1.0
0.8
0.6
0.4
0.2
0.0

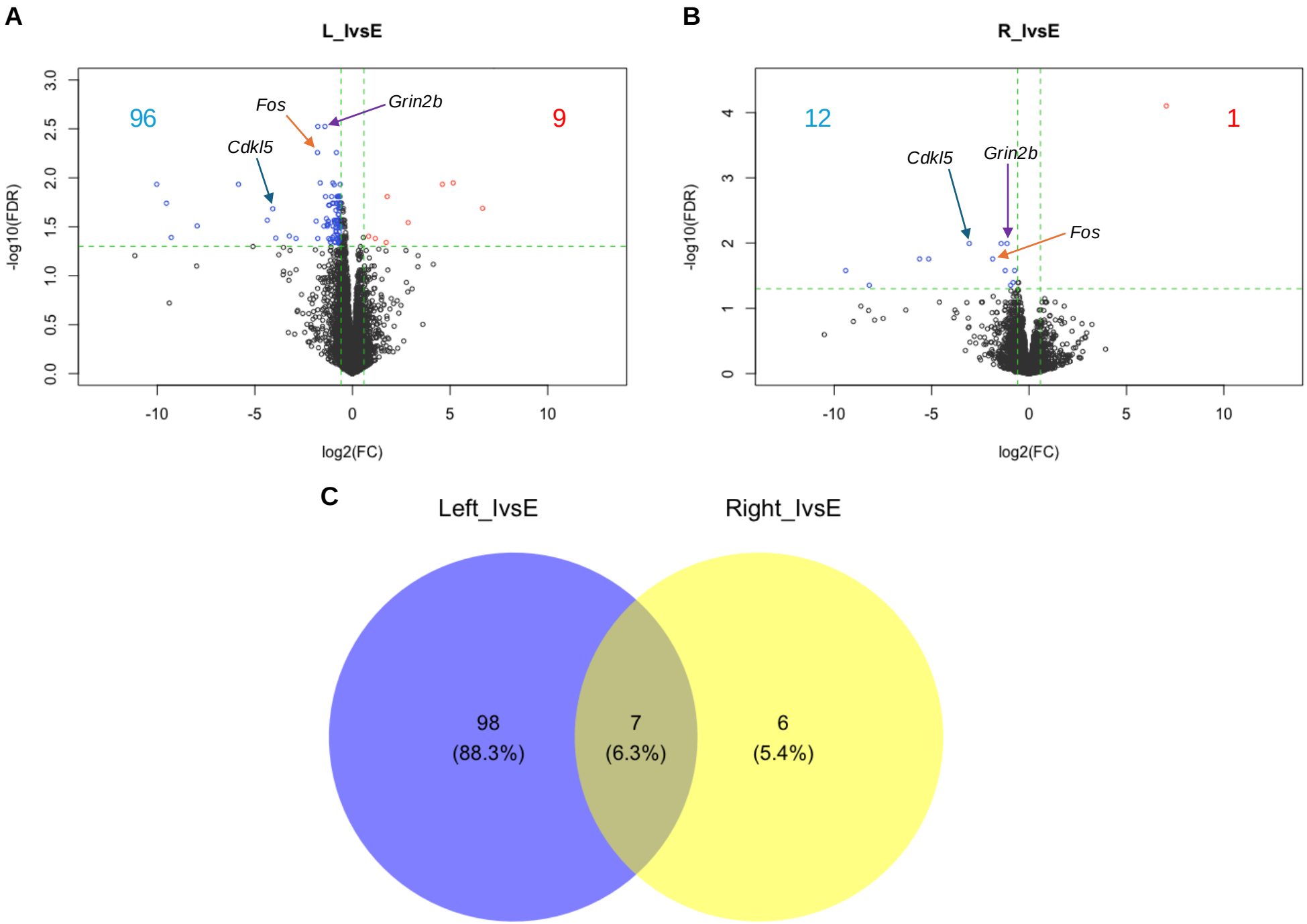
A
L_IvsE
96
9
Fos
Grin2b
Cdkl5
-log10(FDR)
log2(FC)
B
R_IvsE
12
1
Cdkl5
Grin2b
Fos
-log10(FDR)
log2(FC)
C
Left_IvsE
Right_IvsE
98
(88.3%)
7
(6.3%)
6
(5.4%)

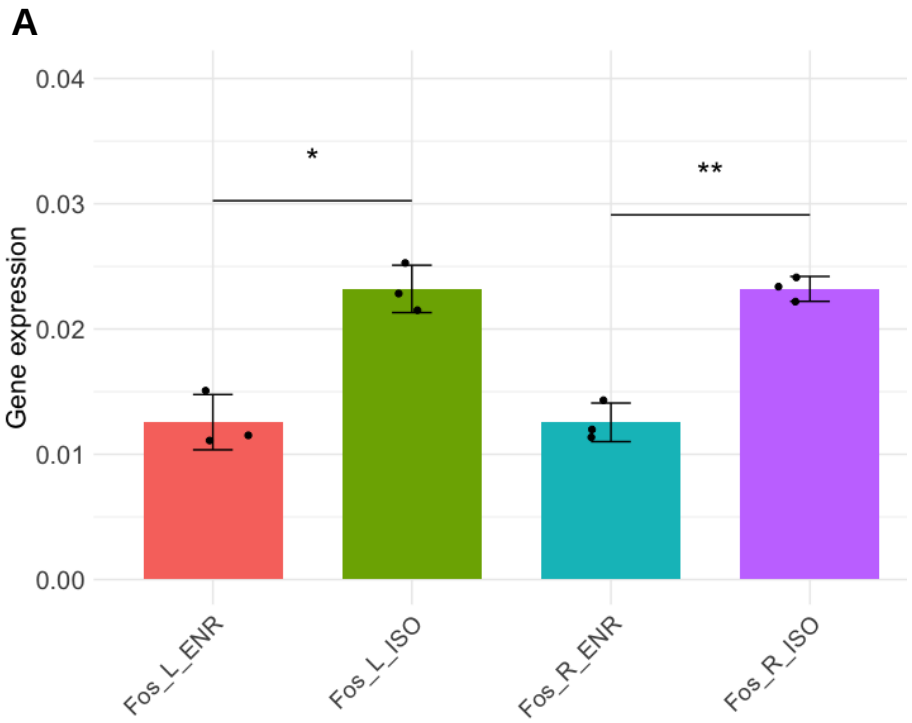
A
0.04
0.03
0.02
0.01
0.00
Gene expression
*
**
Fos_L_ENR
Fos_L_ISO
Fos_R_ENR
Fos_R_ISO

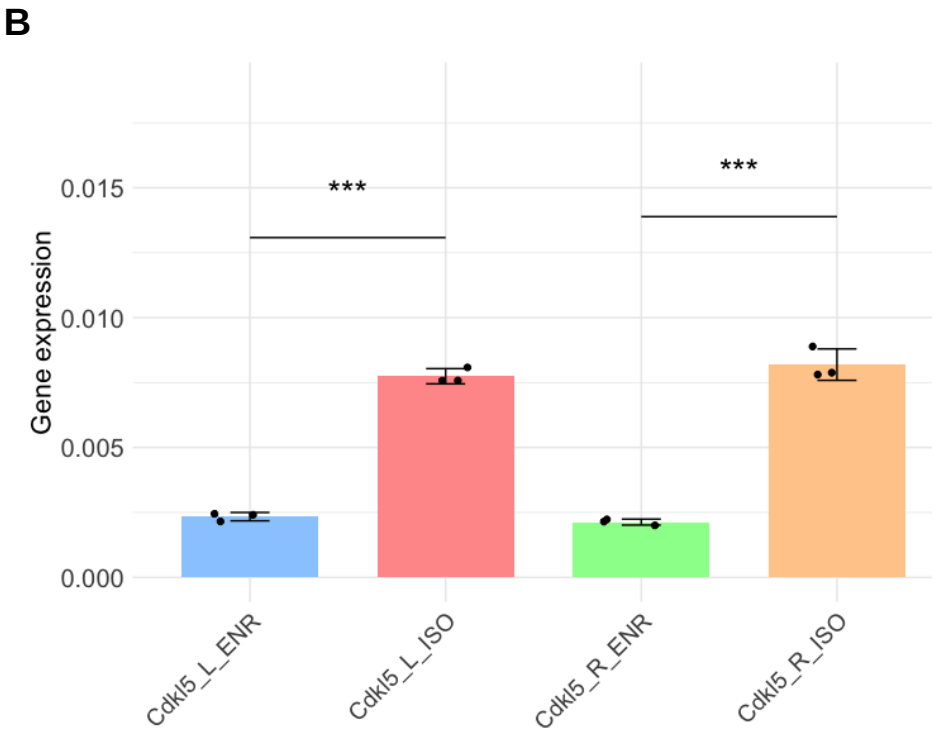
B
0.015
0.010
0.005
0.000
Gene expression
***
***
Cdkl5_L_ENR
Cdkl5_L_ISO
Cdkl5_R_ENR
Cdkl5_R_ISO

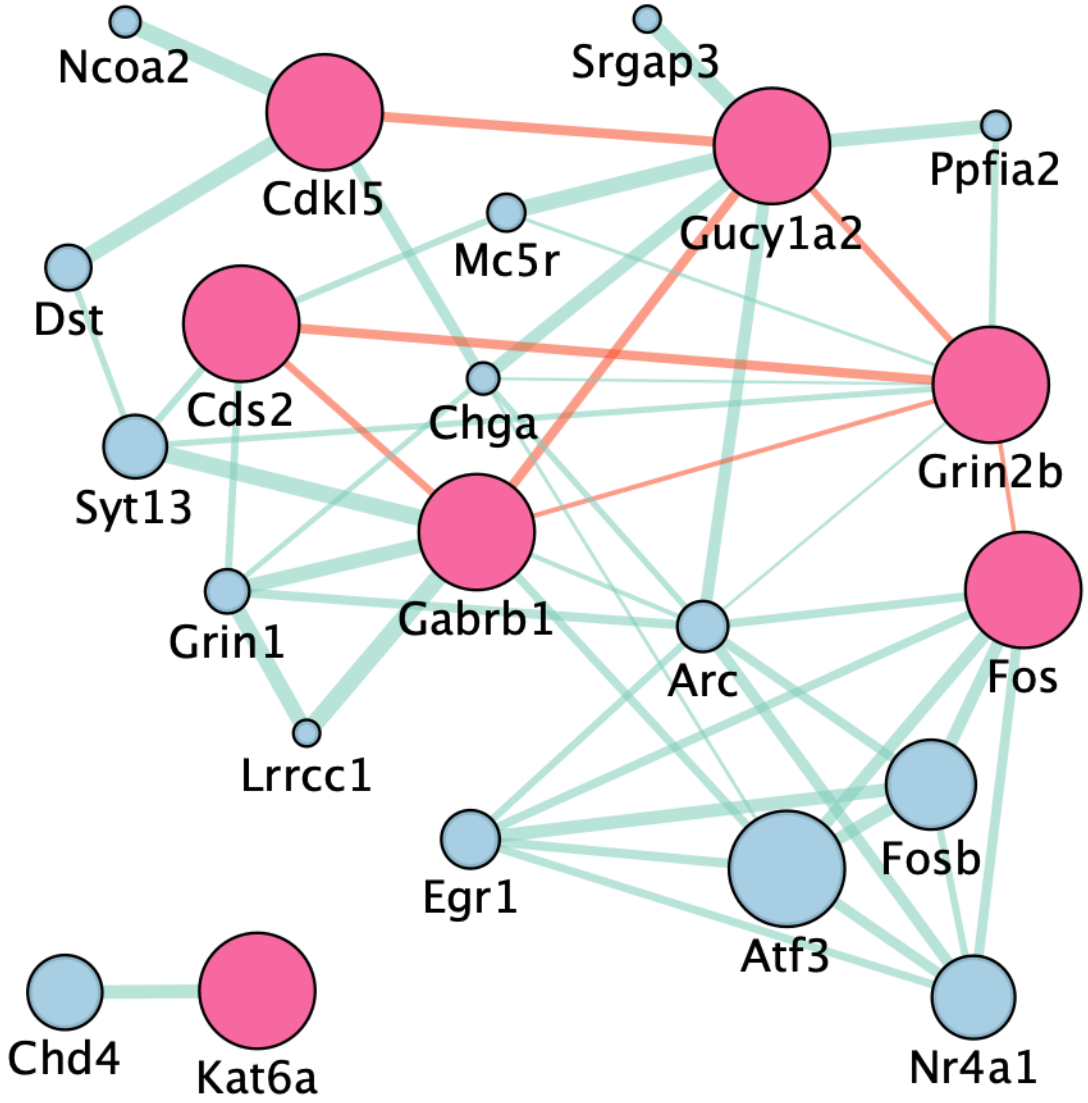
Ncoa2
Srgap3
Cdkl5
Ppfia2
Gucy1a2
Mc5r
Dst
Cds2
Chga
Grin2b
Syt13
Gabrb1
Grin1
Arc
Fos
Lrrcc1
Fosb
Egr1
Atf3
Chd4
Kat6a
Nr4a1

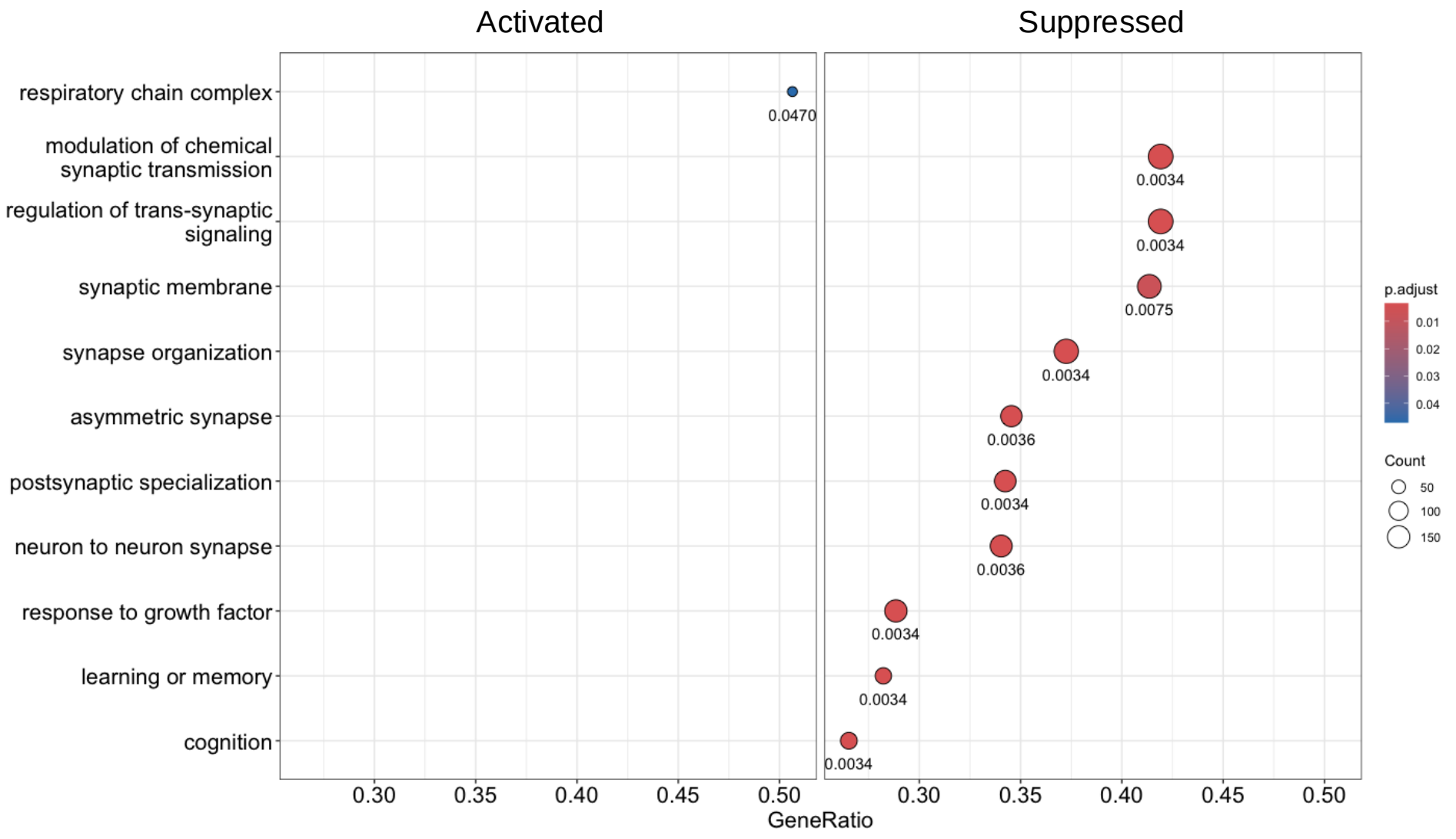
A
Activated
Suppressed
respiratory chain complex
modulation of chemical synaptic transmission
regulation of trans-synaptic signaling
synaptic membrane
synapse organization
asymmetric synapse
postsynaptic specialization
neuron to neuron synapse
response to growth factor
learning or memory
cognition
0.0470
0.0034
0.0034
0.0075
0.0034
0.0036
0.0034
0.0036
0.0034
0.0034
0.0034
0.30
0.35
0.40
0.45
0.50
GeneRatio
p.adjust
0.01
0.02
0.03
0.04
Count
50
100
150

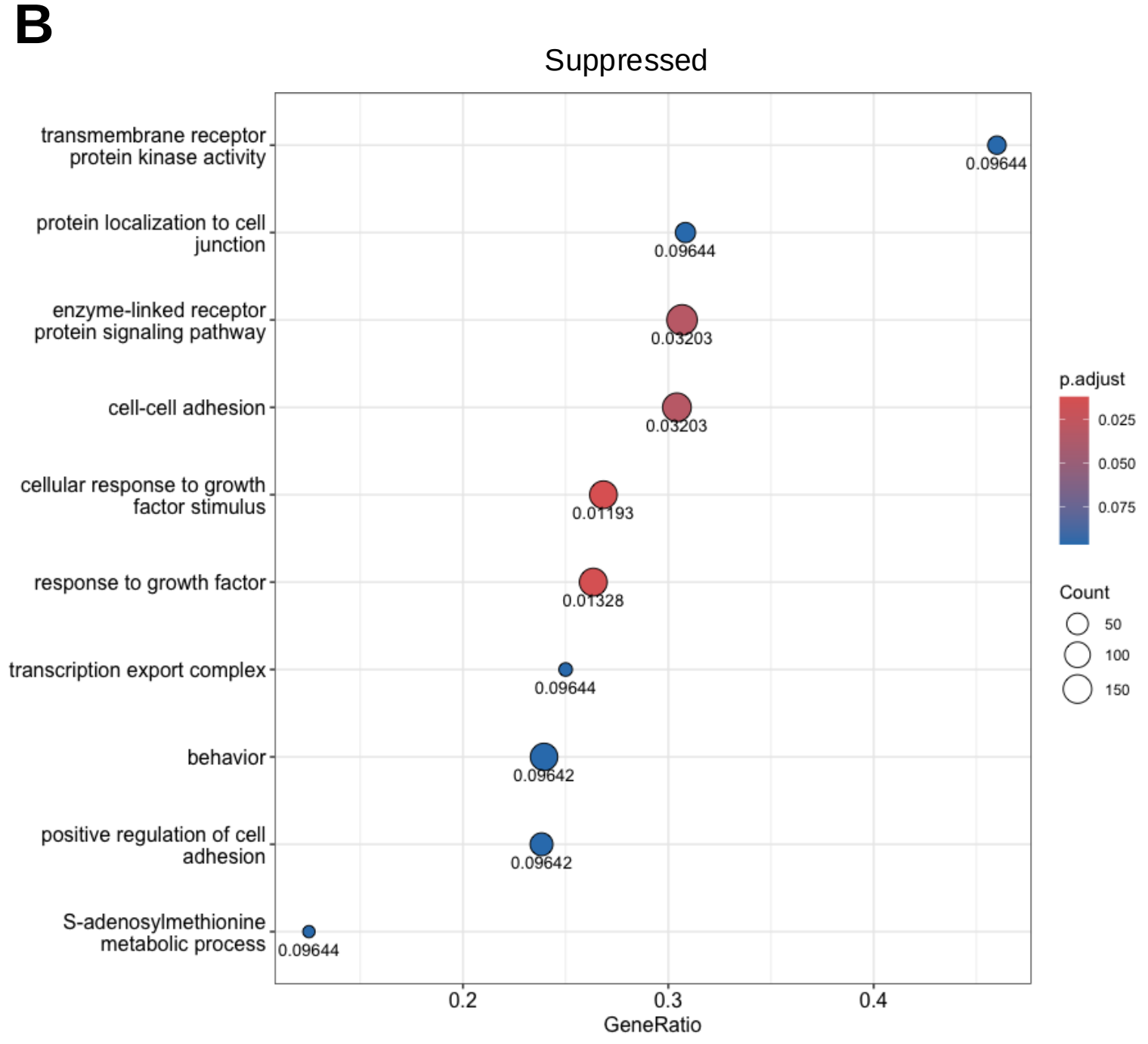
B
Suppressed
transmembrane receptor protein kinase activity
protein localization to cell junction
enzyme-linked receptor protein signaling pathway
cell-cell adhesion
cellular response to growth factor stimulus
response to growth factor
transcription export complex
behavior
positive regulation of cell adhesion
S-adenosylmethionine metabolic process
0.09644
0.09644
0.03203
0.03203
0.01193
0.01328
0.09644
0.09642
0.09642
0.09644
0.2
0.3
0.4
GeneRatio
p.adjust
0.025
0.050
0.075
Count
50
100
150